Solution-phase Synthesis of Cesium Lead Halide Perovskite Nanowires

Dandan Zhang[†,§,❖], Samuel W. Eaton[†,❖], Yi Yu[†], Letian Dou[†,§], Peidong Yang[*,†,‡,§,∥]

[†]Department of Chemistry, [‡]Department of Materials Science and Engineering, University of California, Berkeley, CA 94720, United States

[§]Materials Sciences Division, Lawrence Berkeley National Laboratory, Berkeley, CA 94720, United States

[∥] Kavli Energy Nanosciences Institute, Berkeley, CA 94720, United States

Supporting Information Placeholder

ABSTRACT: H*alide perovskites have attracted much attention over the past five years as a promising class of materials for optoelectronic applications. However, compared to hybrid organic-inorganic perovskites, the study of their pure inorganic counterparts, like cesium lead halides ($CsPbX_3$), lags far behind. Here, a catalyst-free, solution-phase synthesis of $CsPbX_3$ nanowires (NWs) is reported. These NWs are single crystalline with uniform growth direction, and crystallize in the orthorhombic phase. Both $CsPbBr_3$ and $CsPbI_3$ are photoluminescence (PL) active, with composition-dependent temperature and self-trapping behavior. These NWs with a well-defined morphology could serve as an ideal platform for the investigation of fundamental properties and the development of future applications in nanoscale optoelectronic devices based on all-inorganic perovskites.*

Halide perovskites have been demonstrated to be a promising class of materials for optoelectronic applications[1], including high-efficiency photovoltaic cells[1a], light-emitting diodes[1b], lasers[1c], and photodetectors[1d]. The advantages of these compounds include their excellent charge-transport properties[1e] and the broad chemical tunability[1f]. While recent studies have been mostly focused on hybrid organic-inorganic compounds, the study of their inorganic analogues, like AMX_3 (A = Rb, Cs; M = Ge, Sn, Pb; X = Cl, Br, I) is limited[2].

Previous studies on the all-inorganic halide perovskites have revealed that these materials have great potential in optoelectronic applications. $CsGeX_3$ are known for their nonlinear optical properties and potentially useful for nonlinear optics in the mid-infrared and infrared region[2c,2d]. $CsSnI_{3-x}F_x$ has been demonstrated to be an effective hole-transport material and is able to replace the problematic organic liquid electrolytes in dye-sensitized solar cells[2e]. Theoretical calculations on $ASnX_3$ (A = Cs, CH_3NH_3, $NH_2CH{=}NH_2$; X = Cl, I) suggested that their electronic properties strongly depend on the structure of the inorganic SnX_6 octahedral cage[2f], which implies good prospects for the all-inorganic halide perovskites.

However, most of these studies were based on polycrystalline perovksite films deposited on substrates using vapor phase co-evaporation[2e] or solution deposition[2b] of a mixture of AX and BX_2. The uncontrolled precipitation or evaporation of the perovskite produces large morphological variations, making it a non-ideal platform for understanding these materials' fundamental properties.

Controlled synthesis of materials with high quality and well-defined morphology not only benefits fundamental research but also offers great promise for practical applications[3]. Examples include the development of semiconducting quantum dots (QDs)[3a], one-dimensional (1D) NWs[3b], and two-dimensional (2D) nanosheets[3c], which can have superior optical and electrical properties to their bulk counterparts. In terms of inorganic halide perovskites, with the exception of single crystalline QDs[2a], there have been no reports of 1D or 2D nanostructures. Semiconductor NWs, in particular, currently attract widespread interest due to the great potential to advance fundamental and applied research towards new classes of inherently 1D photonic and electronic nanostructures.

Here, a catalyst-free, solution-phase synthesis of $CsPbX_3$ NWs is reported. Detailed structural characterization reveals that these NWs are single crystalline with uniform growth direction and crystalize in an orthorhombic phase. Optical measurements show that both $CsPbBr_3$ and $CsPbI_3$ are PL active, with $CsPbBr_3$ showing strong photoluminescence, $CsPbI_3$ exhibiting a self-trapping effect, and both displaying temperature-dependent photoluminescence. These single-crystalline NWs could serve as an ideal platform for further investigation of structure-function relationships critical to the development of future applications in nanoscale optoelectronics.

Synthesis of $CsPbX_3$ NWs: The preparation of $CsPbX_3$ NWs was performed under air-free conditions using standard Schlenk techniques, by reacting Cs-oleate with Pb-halide in the presence of oleic acid and oleylamine in octadecene (ODE) at 150 - 250 °C. To analyze the NWs formation mechanism, the reaction was quenched to room temperature at different points in time and the respective intermediates were separated by centrifugation and

examined using X-ray diffraction (XRD) and transmission electron microscopy (TEM).

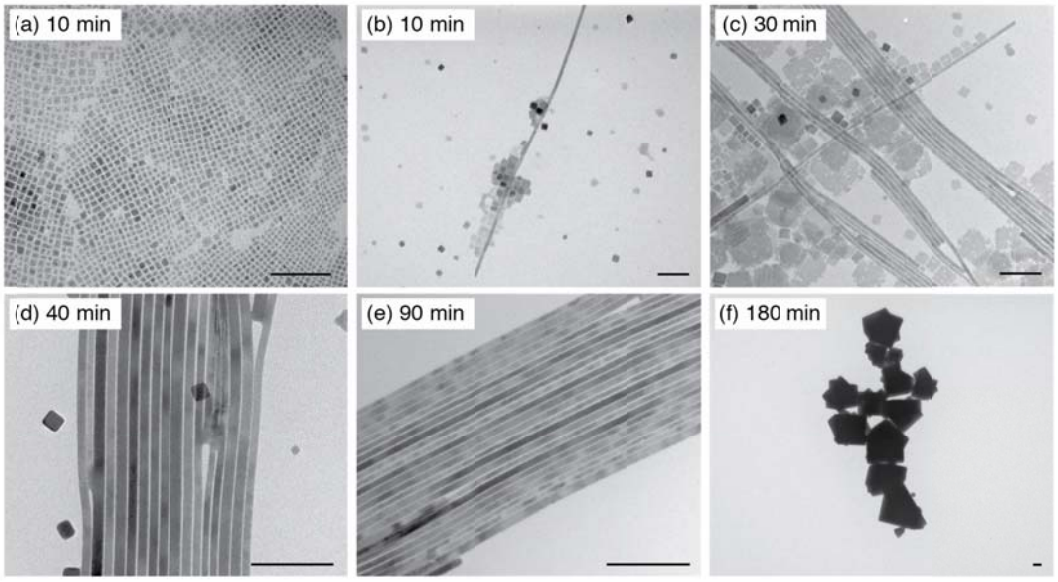

Fig. 1. Shape evolution of the as-prepared $CsPbBr_3$ nanostructures synthesized with different reaction time. Scale bar, 100 nm.

For $CsPbBr_3$ NWs synthesis, the reaction dynamics have been studied at 150 °C. At the initial stage (t < 10 min), the reaction is dominated by the formation of nanocubes (NCs) with size ranging from 3-7 nm (Fig. 1a). After 10 mins, a few of thin NWs with diameters around 9 nm are found in the product (Fig. 1b). With increasing time, more NWs form while the amount of NCs decreases; in addition, there are some square-shaped nanosheets in the product (Fig. 1c, S7a). At a later stage (40 – 60 min) in the reaction, the nanosheets dissolved and NWs with diameters uniformly below 12 nm (Fig. 1d, 1e) and lengths up to 5 μm (Fig. S1a-c) account for a greater proportion of the product, along with the formation of crystals with sizes larger than 200 nm (Fig. S1c). With longer time, the NWs gradually disappear, and the product consists mainly of the large crystals (Fig. 1f). Notably, these morphologies do not represent discrete intermediates formed at specific reaction times, but evolve sequentially from each other. Consequently different intermediates can coexist in the product at a given time during the reaction (Scheme S1). The growth of $CsPbI_3$ NWs requires elevated temperatures (T > 180 °C) and demonstrates much faster kinetics. As such, the reaction is less controllable and the size distribution of the NWs is wider, ranging from tens to hundreds of nanometers (Fig. S2). The $CsPbCl_3$ NWs have also been synthesized at 150 °C, but the proportion of the NWs in the product at different reaction stages is always relatively low (Fig. S3).

Catalyst-free, solution-phase syntheses are commonly used to prepare nanostructures with low aspect ratio such as rods and dots[4]. The formation of high aspect ratio NWs in solution is usually obtained by oriented attachment of nanocrystals[5] or by anisotropic growth driven by high monomer concentrations with the assistance of surfactant capping[4b,6]. We believe that the formation of the $CsPbX_3$ NWs here is not likely due to a dipole driven one-dimensional oriented attachment of NCs[5], since no dimers or 'oligomers' of NCs are observed in the products, and during the aging of colloidal solution of the nanocrystals, there is no nanorod formation due to the dipole driven attachment (Figure S4). In order to get better understanding of NW growth mechanism, more experiments have been conducted to investigate the influence of temperature, time, surfactants, and precursor concentration on the morphology of the product (Table S1). A control experiment done by changing the reaction solvent from ODE to oleylamine shows much slow kinetics but with higher yield of NWs, which suggests the NW formation is most likely through a surfactant-directed 1D growth mode (Supporting Information).

Structural characterization of $CsPbX_3$ NWs: $CsPbX_3$ bulk crystals exhibit a cubic perovskite structure in the highest temperature phase[7]. Upon lowering the temperature, $CsPbI_3$ undergoes one phase transition[7a]: Cubic $\xrightarrow{328\,^{\circ}C}$ orthorhombic, with color changes from dark to yellow[7c]. $CsPbBr_3$ has two phase transitions[7b]: Cubic $\xrightarrow{130\,^{\circ}C}$ tetragonal $\xrightarrow{88\,^{\circ}C}$ orthorhombic, with hardly any color change (orange)[7c]. $CsPbCl_3$ shows three successive phase transitions[7d]: Cubic $\xrightarrow{47\,^{\circ}C}$ tetragonal $\xrightarrow{42\,^{\circ}C}$ orthohombic $\xrightarrow{37\,^{\circ}C}$ monoclinic, with hardly any color change (pale yellow)[7c].

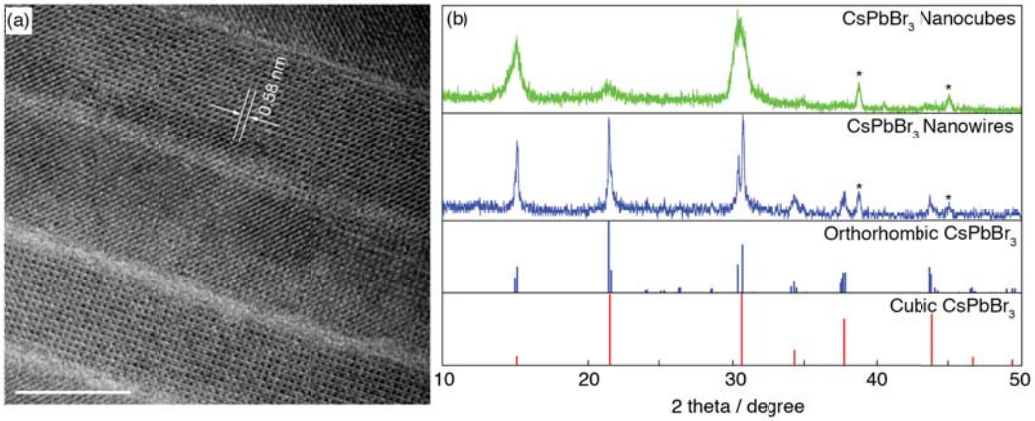

Fig. 2. Structural characterizations of $CsPbBr_3$ NWs. (a) Representative HR-TEM image of $CsPbBr_3$ NWs. Scale bar, 10 nm. (b) Experimental XRD spectrum (top two) of $CsPbBr_3$ NCs and NWs, standard XRD patterns (bottom two) for orthorhombic and cubic phase of $CsPbBr_3$, * labeled extra peaks are caused by the XRD aluminum stage.

Both the yellow color of the crystal (Fig. S5b) and the XRD pattern (Fig. S5b) confirm that the $CsPbI_3$ NWs are in the orthorhombic phase. The HR-TEM images (Fig. S5a) show that the $CsPbI_3$ NWs are single crystalline with uniform <100> growth direction. The phase of $CsPbBr_3$ NWs needs more careful determination because of the small difference between the XRD standard patterns of the orthorhombic and cubic phases. As shown in Fig 2b, the key difference in distinguishing the orthorhombic phase from cubic phase is the double peaks at ~30°. The broadening peak caused by the small size of the $CsPbBr_3$ NCs makes it difficult to determine their exact phase, while the clear double peak at ~30° confirms that the $CsPbBr_3$ NWs are grown in the orthorhombic phase. The HR-TEM images (Fig. 2a, Fig. S6) show that the $CsPbBr_3$ NWs are single crystalline with uniform <110> growth direction. The XRD spectrum of $CsPbBr_3$ nanosheets also suffers severe peak broadening (Fig. S7c), making it difficult to tell its exact phase. Atomic force microscopy (AFM) images show the thickness of the nanosheets ranges from 0.5 – 2 nm (Fig. S8). HR-TEM images of the sheets show lattice patterns with anti-phase boundaries (Fig. S7b), which is commonly observed in oxide perovskites[8]. The exact phase of $CsPbCl_3$ cannot be determined by our X-ray diffractometer because the resolution of the instrument cannot differentiate the closely spaced peaks.

Optical properties of $CsPbX_3$ NWs: The optical properties of the $CsPbX_3$ (X = Br, I) NWs were studied by measuring the UV-Vis absorption and PL spectra of each material dispersed on a substrate (Fig. 3). The absorption onsets for the $CsPbBr_3$ and $CsPbI_3$ NWs were found to be 521 nm (2.38 eV) and 457 nm (2.71 eV), respectively.

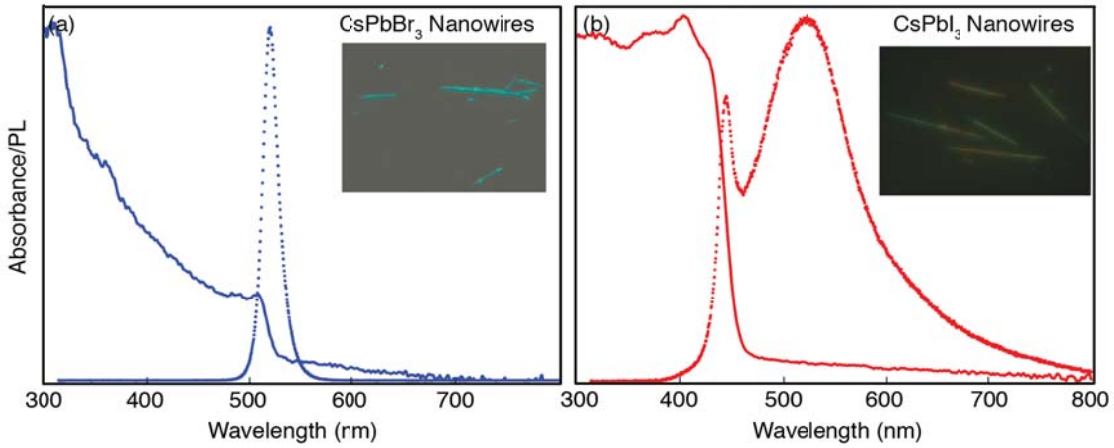

Fig. 3. Optical characterizations of CsPbI3 and CsPbBr3 NWs. (a, b) Typical optical absorption and PL spectra for $CsPbBr_3$ NWs and $CsPbI_3$ NWs, respectively. Inset: optical images of $CsPbBr_3$ and $CsPbI_3$ NWs under the laser beam.

The narrow PL spectrum of $CsPbBr_3$ (Fig. 3a, dotted line) corresponds to excitonic emission with a small degree of quantum confinement (60 meV blue-shift, Fig. S10) due to the narrow wire diameter. A greater degree of confinement is observed for the nanosheets (69 meV) due to an average sheet thickness of only a few unit cells (Fig. S9). Temperature-dependent PL of the $CsPbBr_3$ NWs reveals a small blue-shift (0.035 meV/K) with increasing temperature (Fig. S11). While the opposite trend is typically observed, this behavior has been reported for a range of materials including Pb-doped CsBr crystals[9] as well as closely related cesium metal halide[10] and organometal halide pervoskites[11]. The effect is attributed to the balance between lattice expansion/contraction and electron-phonon coupling; electron-phonon coupling typically dominates band gap behavior and results in a red-shift with increasing temperature. Yu et al. reported,

however, that the lattice term was dominant in $CsSnI_3$[10]; we hypothesize that $CsPbBr_3$ behaves similarly here.

Our $CsPbI_3$ PL spectrum (Fig. 3b, dotted line) consists of two distinct peaks centered at 446 nm (2.78 eV) and 523 nm (2.37 eV) with widths of 115 meV and 530 meV (FWHM), respectively. The narrow, high-energy peak likely stems from excitonic emission similar to $CsPbBr_3$, but the broad, low-energy peak observed for $CsPbI_3$ has been attributed previously to the formation of self-trapped excitons (STE)[12]. Exciton self-trapping has been observed for a variety of ionic compounds including a number of recently studied organometal halide perovskite materials[11a,13]. The temperature-dependent PL of $CsPbI_3$ NWs is also significantly more complex than $CsPbBr_3$ (Fig. S11). At low temperatures, only STE emission is observed. Upon heating past 100 K, the excitonic emission peak appears and grows monotonically with temperature. Unlike $CsPbBr_3$, the excitonic peak red-shifts with increasing temperature, suggesting that strong electron-phonon coupling contribution dictates band gap behavior. This is consistent with the self-trapping of excitons; increased electron-phonon coupling results in greater lattice distortion in the proximity of the exciton, thereby increasing the probability of trapping[13a]. Additional PL discussion may be found in the SI (Table S2).

In summary, a catalyst-free, solution-phase synthetic approach has been developed to obtain single crystalline, orthorhombic $CsPbX_3$ NWs with uniform growth direction. Optical studies determined that both $CsPbBr_3$ and $CsPbI_3$ are PL active, and exhibit both unique compositional and temperature-dependent behavior. Future studies with these NWs will concentrate on the investigation of their electronic and thermoelectronic properties as well as the development of their optoelectronic applications. Additionally, while this work focuses on the $CsPbX_3$ class of compounds, the synthetic method reported here can potentially be applied to other inorganic perovskites, such as tin-based perovskites, which will be less toxic.

ASSOCIATED CONTENT

Supporting information

Experimental details, additional TEM, XRD, UV-vis and PL data. This material is available free of charge via the Internet at http://pubs.acs.org.

AUTHOR INFORMATION

Corresponding Author

p_yang@berkeley.edu.

Author Contributions

❖These authors contributed equally to this work.

Notes

The authors declare no competing financial interest.

ACKNOWLEDGMENT

This work was supported by the Director, Office of Science, Office of Basic Energy Sciences, Materials Science and Engineering Division, U.S. Department of Energy under Contract No. DE-AC02-05CH11231 (PChem). S.W.E would like to thank the Camille and Henry Dreyfus Foundation for funding, award no. EP-14-151.

REFERENCES

(1) (a) Liu, M.; Johnston, M. B.; Snaith, H. J. *Nature*, **2013**, 501, 395. (b) Tan, Z.-K.; Moghaddam, R. S.; Lai, M. L.; Docampo, P.; Higler, R.; Deschler, F.; Price, M.; Sadhanala, A.; Pazos, L. M.; Credgington, D.; Hanusch, F.; Bein, T.; Snaith, H. J.; Friend, R. H. *Nat Nano.* **2014**, 9, 687. (c) Zhang, Q.; Ha, S. T.; Liu, X.; Sum, T. C.; Xiong, Q. *Nano Lett.* **2014**, 14, 5995. (d) Dou, L.; Yang, Y. M.; You, J.; Hong, Z.; Chang, W. H.; Li, G.; Yang, Y. *Nat. Commun.* **2014**, 5, 5404. (e) Dong, Q.; Fang, Y.; Shao, Y.; Mulligan, P.; Qiu, J.; Cao, L.; Huang, J. *Science,* **2015**, *347*, 967. (f) Noh, J. H.; Im, S. H.; Heo, J. H.; Mandal, T. N.; Seok, S. I. *Nano Lett.* **2013**, *13*, 1764.

(2) (a) Protesescu, L.; Yakunin, S.; Bodnarchuk, M. I.; Krieg, F.; Caputo, R.; Hendon, C. H.; Yang, R. X.; Walsh, A.; Kovalenko, M. V. *Nano Lett.* **2015,** 15, 3692. (b) Chung, I.; Song, J.-H.; Im, J.; Androulakis, J.; Malliakas, C. D.; Li, H.; Freeman, A. J.; Kenney, J. T.; Kanatzidis, M. G. *J. Am. Chem. Soc.* **2012**, *134*, 8579. (c) Tang, L. C.; Huang, J. Y.; Chang, C. S.; Lee, M. H.; Liu, L. Q. *J. Phys. Condens. Matter,* 2005, 17, 7275. (d) Li-Chuan, T.; Yia-Chung, C.; Jung-Yau, H.; Ming-Hsien, L.; Chen-Shiung, C. *Jpn. J. Appl. Phys.* 2009, 48, 112402. (e) Chung, I.; Lee, B.; He, J.; Chang, R. P. H.; Kanatzidis, M. G. *Nature,* **2012**, *485*, 486. (f) Borriello, I.; Cantele, G.; Ninno, D. *Phys. Rev. B*, **2008**, *77*, 235214.

(3) (a) Alivisatos, A. P. *Science,* **1996**, *271*, 933. (b) Huang, M. H.; Mao, S.; Feick, H.; Yan, H.; Wu, Y.; Kind, H.; Weber, E.; Russo, R.; Yang, P. *Science,* **2001**, *292*, 1897. (c) Wang, Q. H.; Kalantar-Zadeh, K.; Kis, A.; Coleman, J. N.; Strano, M. S. *Nat. Nano.* **2012**, *7*, 699.

(4) (a) Peng, X.; Manna, L.; Yang, W.; Wickham, J.; Scher, E.; Kadavanich, A.; Alivisatos, A. P. *Nature,* **2000**, *404*, 59. (b) Peng, Z. A.; Peng, X. *J. Am. Chem. Soc.* **2002**, *124*, 3343.

(5) Cho, K. S.; Talapin, D. V.; Gaschler, W.; Murray, C. B. *J. Am. Chem. Soc.* **2005**, 127, 7140.

(6) Xi, L.; Tan, W. X. W.; Boothroyd, C.; Lam, Y. M. *Chem. Mater.* **2008**, *20*, 5444.

(7) (a) Trots, D. M.; Myagkota, S. V. *J. Phys. Chem. Solids,* **2008**, 69, 2520. (b) Sakata, M.; Nishiwaki, T.; Harada, J. *J. Phys. Soc. Jpn.* **1979**, 47, 232. (c) Moller, C. K. *Nature,* **1958**, 182, 1436. (d) Fujii, Y.; Hoshino, S.; Yamada, Y.; Shirane, G. *Phys. Rev. B,* **1974**, 9, 4549.

(8) Van Tendeloo, G.; Lebedev, O. I.; Amelinckx, S. *J. Magn. Magn. Mater.* **2000**, *211*, 73.

(9) Aceves, R.; Babin, V.; Flores, M. B.; Fabeni, P.; Maaroos, A.; Nikl, M.; Nitsch, K.; Pazzi, G. P.; Salas, R. P.; Sildos, I.; Zazubovich, N.; Zazubovich, S. *J. Lumin.* **2001**, 93, 27.

(10) Yu, C.; Chen, Z.; J. Wang, J.; Pfenninger, W.; Vockic, N.; Kenney, J. T.; Shum, K. *J. Appl. Phys.* **2011**, *110*, 063526.

(11) (a) Dohner, E. R.; Jaffe, A.; Bradshaw, L. R.; Karunadasa, H. I. *J. Am. Chem. Soc.* **2014**, *136*, 13154. (b) Wu, K.; Bera, A.; Ma, C.; Du, Y.; Yang, Y.; Li, L.; Wu, T. *Phys. Chem. Chem. Phys.* **2014**, *16*, 22476.

(12) (a) Nikl, M.; Nitsch, K.; Somma, F.; Fabeni, P.; Pazzi, G. P.; Feng, X. Q. *J. Lumin.* **2000**, *87–89*, 372. (b) Babin, V.; Fabeni, P.; Nikl, M.; Nitsch, K.; Pazzi, G. P.; Zazubovich, S. *Phys. Status solidi (b),* **2001**, *226*, 419.

(13) (a) Williams, R. T.; Song, K. S. *J. Phys. Chem. Solids,* **1990**, *51*, 679. (b) Wu, X.; Trinh, M. T.; Niesner, D.; Zhu, H.; Norman, Z.; Owen, J. S.; Yaffe, O.; Kudisch, B. J.; Zhu, X. Y. *J. Am. Chem. Soc.* **2015**, *137*, 2089.

Table of Content Graphic